Safety and Health at Work 13 (2022) 315–325

Contents lists available at ScienceDirect

Safety and Health at Work

journal homepage: www.e-shaw.net

Original article

Musculoskeletal Model for Assessing Firefighters' Internal Forces and Occupational Musculoskeletal Disorders During Self-Contained Breathing Apparatus Carriage

Shitan Wang [1,2,3], Yunyi Wang [3,4,*]

[1] Shanghai Yangzhi Rehabilitation Hospital (Shanghai Sunshine Rehabilitation Center), School of Medicine, Tongji University, Shanghai, 201619, China
[2] Department of Rehabilitation Sciences, School of Medicine, Tongji University, Shanghai, 201619, China
[3] College of Fashion and Design, Donghua University, Shanghai, 200051, China
[4] Key Laboratory of Clothing Design and Technology (Donghua University), Ministry of Education, Shanghai, 200051, China

ARTICLE INFO

Article history:
Received 31 October 2021
Received in revised form
3 March 2022
Accepted 22 March 2022
Available online 28 March 2022

Keywords:
biomechanical evaluation
firefighters
grey relation analysis
musculoskeletal disorders
personal protective equipment

ABSTRACT

Background: Firefighters are required to carry self-contained breathing apparatus (SCBA), which increases the risk of musculoskeletal disorders. This study assessed the newly recruited firefighters' internal forces and potential musculoskeletal disorders when carrying SCBA. The effects of SCBA strap lengths were also evaluated.

Methods: Kinematic parameters of twelve male subjects running in a control condition with no SCBA equipped and three varying-strapped SCBAs were measured using 3D inertial motion capture. Subsequently, motion data and predicted ground reaction force were inputted for subject-specific musculoskeletal modeling to estimate joint and muscle forces.

Results: The knee was exposed to the highest internal force when carrying SCBA, followed by the rectus femoris and hip, while the shoulder had the lowest force compared to the no-SCBA condition. Our model also revealed that adjusting SCBA straps length was an efficient strategy to influence the force that occurred at the lumbar spine, hip, and knee regions. Grey relation analysis indicated that the deviation of the center of mass, step length, and knee flexion-extension angle could be used as the predictor of musculoskeletal disorders.

Conclusion: The finding suggested that the training of the newly recruits focuses on the coordinated movement of muscle and joints in the lower limb. The strap lengths around 98-105 cm were also recommended. The findings are expected to provide injury interventions to enhance the occupational health and safety of the newly recruited firefighters.

1. Introduction

Musculoskeletal injuries (MSDs) in firefighters, such as sprain, strain, and muscle pains, are the most common on-duty injuries (43–62% of all injuries), which is greater than burn injuries (7%), thermal stress (6%), and toxic gas inhalation (4%) [1,2]. Accidents due to MSDs typically account for the longer work absences for firefighters and higher medical costs than other injuries [3]. The high incidence of firefighters' MSDs is attributed to the excessive joint force and muscle tension to counteract load acts on the musculoskeletal system (bone, nerve, tendon, muscle, and ligament), which generates microscopic fatigue damage in the form of cellular and extracellular degeneration. In particular, the newly recruited firefighters who have no work and training experience were 10 times more likely to be injured than a more experienced firefighter due to a mismatch in physical capability versus applied tissue loading [4]. Therefore, injury assessment and interventions focused on the newly recruited firefighters are necessary.

Biomechanical risk factors for causing MSDs include load carriage, awkward posture, forceful exertion, and repetitive movements [5]. Several studies have reported that firefighters' MSDs are influenced by heavy and bulky personal protective equipment

Shitan Wang: https://orcid.org/0000-0002-6619-8908
* Corresponding author. College of Fashion and Design, Donghua University, Shanghai, 200051, China. Fax: +862162379188.
E-mail address: wangyunyi@dhu.edu.cn (Y. Wang).

2093-7911/$ – see front matter
https://doi.org/10.1016/j.shaw.2022.03.009

(PPE) [6,7]. The PPE consists of turnout garments, self-contained breathing apparatus (SCBA), fire boots, helmet, and gloves, adding a significant physical burden during firefighting and leading to restricted mobility and musculoskeletal injuries in different body regions. The lower back, shoulder, knee, and ankle were all reported as the individual areas of injury for firefighters. SCBA (between 12 and 18 kg) is the heaviest item of firefighters' PPE, which must be carried during both training and firefighting. Heavy SCBA directly exerts a force on the torso and shoulder and causes perceived discomfort, fatigue, and even injury, for example, rucksack palsy and low back problems [8]. Moreover, SCBA carriage during activities alters firefighters' body kinematics, such as reducing step length, increasing hip and knee flexion range of motion (ROM), and increasing center of mass (COM) deviation, which would disturb the normal loading pattern placed on the lower limb [9,10].

To alleviate the biomechanical impacts of SCBA carriage, researchers reduced the weight of SCBA cylinders or redesigned SCBA systems [11]. However, a lighter SCBA cylinder provides limited breathing air capacity, while a low-profile SCBA is high-cost and impractical for each firefighter. Most firefighters currently carry a traditional SCBA system designed with a single-cylinder composed of carbon fiber and aluminum and carried on a frame with a shoulder strap, hip belt, and chest belt. When the SCBA weight is inevitable, variation of SCBA strap lengths to alter the weight distribution on the body may be an alternative solution.

Although the incidence of MSDs in firefighters is high, to date, firefighters' injury studies are limited to the epidemiological investigation [12,13], quantitatively assessment of firefighters' loading is rarely performed, and the kinematic changes that are indicative of eventual injury is also unknown. One challenge is that noninvasive measurement of *in vivo* muscle, bone, and joint forces, is still impossible due to technical and ethical restrictions. Recently, computer-based musculoskeletal models have been developed to estimate joint and muscle forces by solving the force equilibrium equations with inverse dynamics analysis; however, musculoskeletal models related to firefighters have not been developed.

Therefore, the purpose of this study was to quantify the effects of SCBA carriage and the adjustment of strap lengths on newly recruited firefighters' internal joint and muscle forces by developing musculoskeletal models. The kinematic index most strongly related to the kinetic responses was also determined, expected to be a predictor variable of potential MSDs. The findings of our study were expected to develop injury intervention strategies to optimize firefighters' work safety.

2. Materials and methods

2.1. Motion capture experiment

A motion capture experiment was conducted to obtain body kinematics. These kinematic data were used as inputs for full-body musculoskeletal modeling. Electromyography signal (EMGs) was synchronously collected with kinematic data and as the validation data of musculoskeletal simulation.

2.1.1. Participants and inclusion criteria

The sample size was determined by power analysis using G*Power 3.1 software. A repeated ANOVA test was used, the effect size set to be 0.6 (this value was calculated using the means and standard deviations within each group), alpha set to be 0.05, and power set to be 0.8. The corresponding sample size was calculated as eight. Twelve healthy males (age: 23.1 ± 2.1 years, height: 174.6 ± 2.4 cm, mass: 67 ± 3.5 kg, BMI = 22 ± 1, body fat percentage = 16.5 ± 3.4 %) were finally recruited in the experiment. Their basic information is shown in Table 1.

Table 1
Basic information of subjects

No.	Age (years)	Height (cm)	Mass (kg)	BMI	body fat percentage (%)
1	24.0	173.0	60.9	20.3	15.5
2	21.0	170.2	66.2	22.9	16.2
3	25.0	176.0	71.8	23.2	11.7
4	25.0	173.0	63.3	21.2	18.1
5	23.0	175.0	72.6	23.7	21.2
6	22.0	173.5	70.0	23.3	24.4
7	20.0	178.0	67.1	21.2	14.8
8	26.0	178.0	70.1	22.1	20.3
9	24.0	177.0	66.9	21.4	13.8
10	25.0	171.0	63.7	21.8	13.6
11	22.0	176.0	68.5	22.1	14.5
12	20.0	174.0	64.0	21.1	16.0
Mean	23.1 ± 2.1	174.6 ± 2.4	67.0 ± 3.5	22.0 ± 1.0	16.5 ± 3.4

These recruited subjects are the candidate of the firefighters and meet or exceed the standard of GBZ221-2009 (Standard on occupational health for firefighters) and the Chinese Army Basic Fitness Assessment, including (i) 18 ≤age≤26, (ii) height ≥162 cm, (iii) mass ≤20% of standard body mass (standard body mass = height-110cm), (iv) 17.5 = BMI<30, (v) achieving a minimum of 35 push-ups in 2 minutes, and (vi) achieving a minimum of 5 single-leg squat ups. All subjects were healthy, nonsmokers, and with no history of musculoskeletal or cardiopulmonary conditions. The research was approved by the Institutional Review Board (IRB) from the Colorado State University (IRB No. 19-8876H). All the subjects provided written informed consent before participation.

Prior to the formal experiment, each subject was asked to wear full PPE and perform movement tasks for one week to familiarize themselves with PPE.

2.1.2. Test sample

The PPE used meets GA621-2006, including turnout jacket, pants, gloves, helmet, and SCBA. The turnout gear was a three-layer construction composed of an outer heat-resistant shell, an inner water-resistant moisture barrier layer, and a thermal liner. All recruited subjects were of an average build, and thus the same size (175A) of turnout gear was offered to them. Multiple sizes of new running shoes and gloves with the same style were offered to each subject. Each subject offered a suitable size of new running shoes and gloves with the same style.

Four sets of test samples were examined in this study (Fig. 1), including three kinds of SCBA carriage with different strap lengths (loose-fitting, medium-fitting, and tight-fitting) and a control condition (CC) without SCBA equipped. The level of strap lengths was determined according to previous survey results [1].

2.1.3. Experimental protocol

Full-body 3D kinematic data were collected using the inertial motion capture systems (IMC)-Xsens MVN (Xsens Technologies B.V., Enschede, the Netherlands), sampling at 120 Hz, synchronously with EMGs using a Noraxon system (Noraxon, Scottsdale, Arizona, USA), sampling at 120 Hz. Xsens MVN is a commercially IMC system, and its reliability and accuracy in measuring human ROM are supported by previous studies [14,15].

The experimental procedure and setting are shown in Fig. 2. Firstly, subjects were instructed to wear Xsens Lycra test suits, with 17 Xsens motion sensors fitted to specific positions (head, sternum, pelvis, upper legs, lower legs, feet, shoulders, upper arms, forearms, and hands). Subjects' anthropometric data,

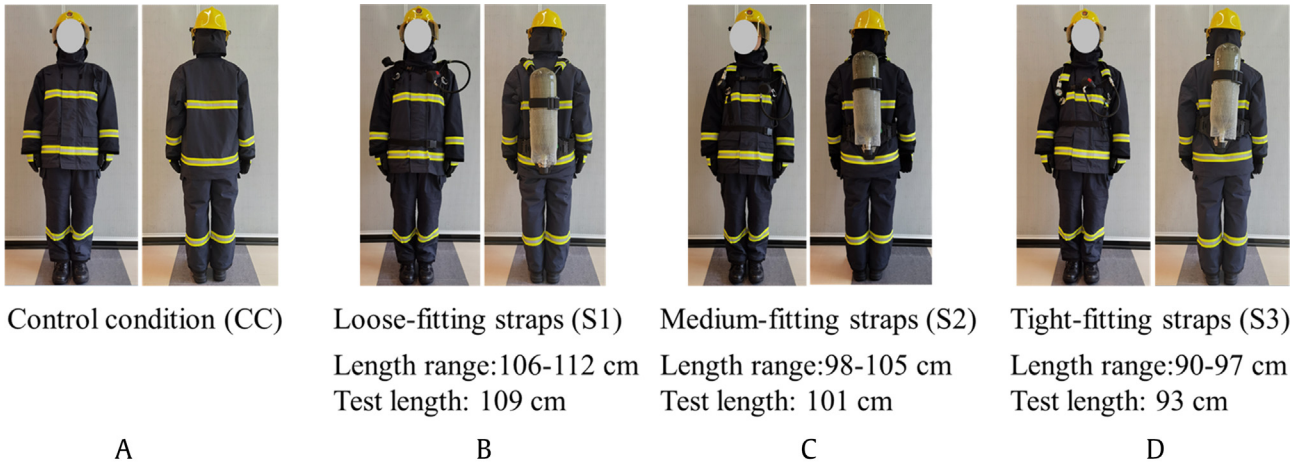

Fig. 1. SCBA strap conditions. (A) Control condition; (B) Loose-fitting strap; (C) Medium-fitting strap; (D) Tight-fitting strap.

including the heights of the ankle, knee, hip, and top of the head from the ground, the widths of the shoulder and pelvis, as well as the length of the foot, were manually measured using a flexible tape (Deli, Ningbo, Zhejiang, China) with the subject in an upright posture. The anthropometric data were then entered into the Xsens MVN software to calibrate the IMC system using a steady,

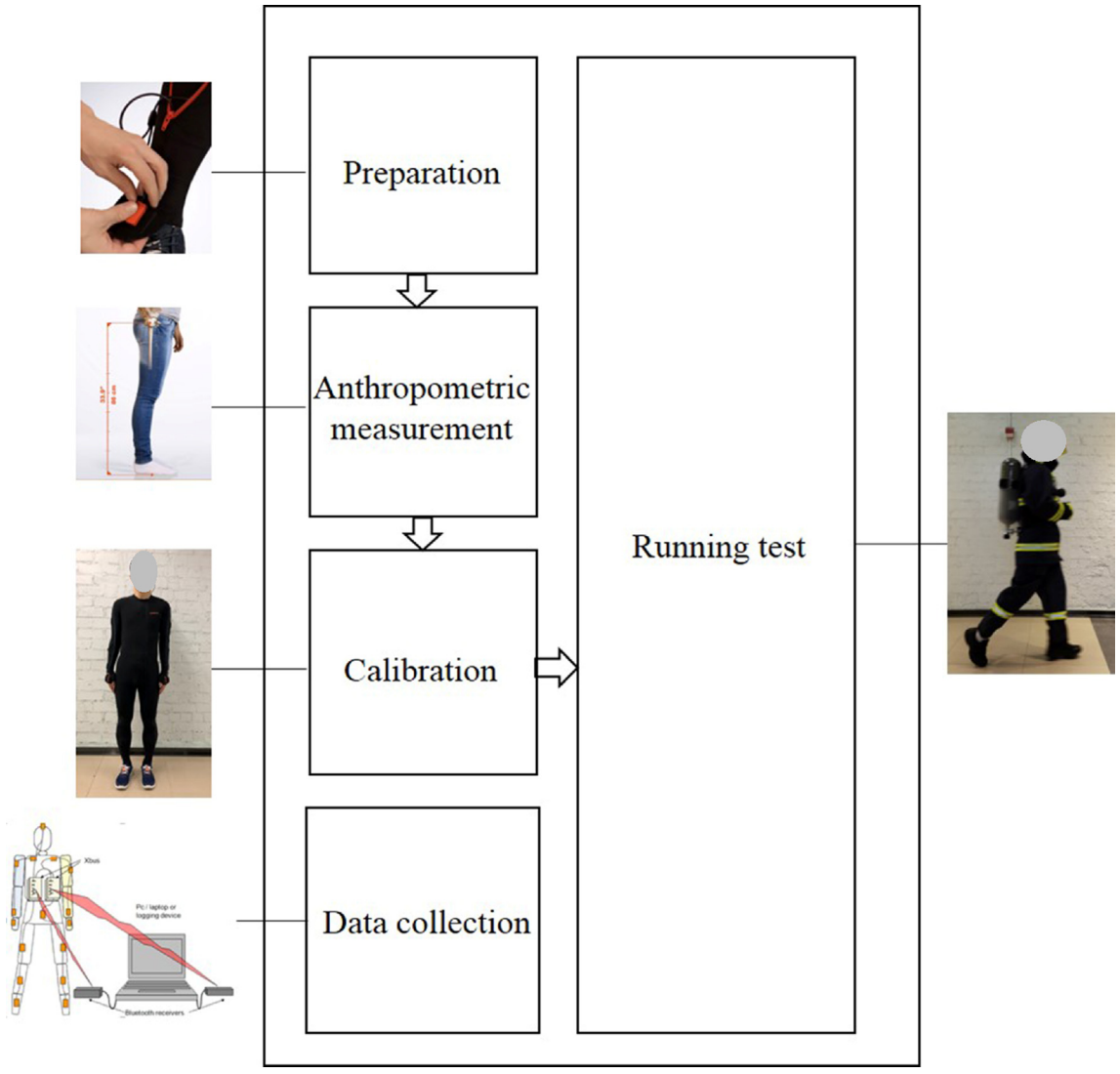

Fig. 2. Experiment procedure and setting.

upright posture. Subsequently, subjects were required to change into the test sample assigned for the day and keep an upright standing neutral position (N-pose) to calibrate the IMC system. After completing the calibration, subjects were asked to run along a 50 m runway at a speed of 4.15 ± 0.25 m/s. The measurement speed was designed to obtain a high metabolic rate level, representing a firefighter's underlying physical conditioning levels needed to perform daily training and job-related physical tasks according to the ISO 7243 standard. Running speed was monitored using a stopwatch. All subjects were asked to begin running with their left foot to ensure consistency. Three repetitions were performed for each test sample in a randomized order, totaling twelve trials for each subject.

2.2. Biomechanical modeling

AnyBodyTM Modeling System (AMS) (version 7.12.2, AnyBodyTM Technology A/S, Aalborg, Denmark) was used to perform musculoskeletal analyses. The modeling process is shown in Fig. 3, including subject-specific model development, kinematic analysis, inverse dynamics calculation, and validation. We performed the musculoskeletal analysis for running with four test samples, and twelve subjects' trials were all involved in modeling.

2.2.1. Subject-specific model development

Subject-specific musculoskeletal models for twelve subjects were developed by scaling the GaitFullBody template in AnyBody Managed Model Repository (AMMR) using the length-mass-scaling law [16].

For each subject, a Biovision Hierarchy (BVH) file (which contains a standing model and absolute position, orientation, velocity, joint angles, etc. for each time frame) was exported from Xsens MVN Studio and imported in AMS, in which a stick figure model was initially constructed with virtual markers. The segment lengths in the template model were scaled according to the joint-to-joint distances of the stick figure model using the measured body dimensions. The total body mass of each subject-specific model was set as the subject's actual body mass. The total body mass was distributed to the individual segments using the regression equations of Winter [17]. The muscle strength was scaled by calculating the muscle strength scaling factor (Eq. (1)).

$$\begin{cases} Strength\ Scaling = Mass\ Scaling \times \dfrac{1 - R_{other} - R_{fat}}{1 - R_{other} - R_{fat0}} \\ R_{fat} = 100 \times \left(-0.09 + 0.0149 \times BMI - 0.00009 \times BMI^2 \right) \\ BMI = Mass \Big/ Length^2 \end{cases} \tag{1}$$

where *Mass Scaling* is the ratio between the subject's body mass and the template body mass; R_{fat} is the fat percentage of each subject; R_{fat0} is the fat percentage of the template model; R_{other} is the mass of other body organs except bones, muscles, and fats, and was set to 0.5; *Mass* and *Length* are the subjects' body weight and height, respectively.

In addition, a simplified SCBA model was developed and interacted with the human model to mimic the actual SCBA carriage. The SCBA model was designed in SOLIDWORKS (version 2016, Dassault Systemes, Massachusetts, USA) and converted to the corresponding AnyScript model using the plug-in AnyExp4SOLIDWORKS™. For driving the SCBA model to run properly with the human model, a code was added to the SCBA model in close proximity to the initial human posture. Kinematic analysis was performed to check the initial state of the human model.

2.2.2. Kinematics analysis and ground reaction force prediction

Once the model was constructed, the model was run for formal kinematic analysis and GRF prediction. The subject's joint angles obtained from the motion capture experiment were used for running the model. The GRF was predicted from kinematics input using the method of Karatsidis et al. [18].

2.2.3. Inverse dynamics calculation

The last step was to run the inverse dynamic analysis, which added the muscles into the model and then established the internally generated kinetics for each time step of the motion. The muscle model was set as AnyMuscleModel3E, which is a three-element model taking serial and parallel elastic elements into account, along with fiber length and contraction velocity. During this

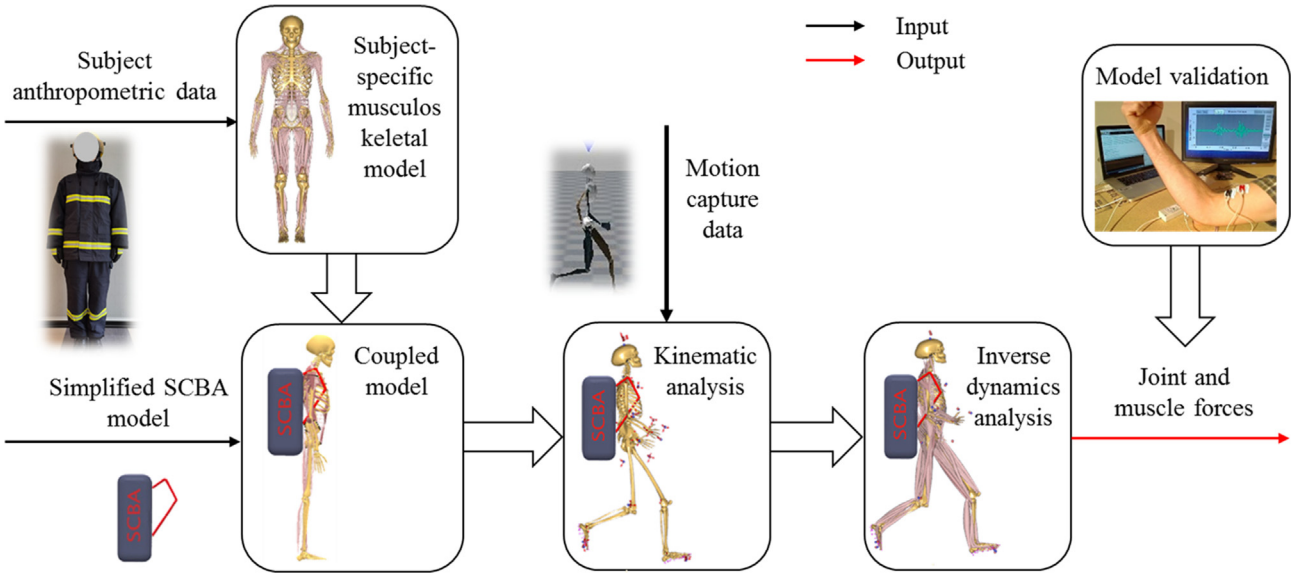

Fig. 3. Process of musculoskeletal modeling.

process, the muscle redundancy problem was solved according to a third-order polynomial optimization.

Minimize function:

$$G\left(f^{(M)}\right) = \sum_{i=1}^{n^{(M)}} \left(\frac{f_i^{(M)}}{N_i}\right)^3 \quad (2)$$

Subject to:

$$Cf = d \quad (3)$$

$$f_i^{(M)} \geq 0,\ i \in \left\{1, 2 \ldots\ldots n^{(M)}\right\} \quad (4)$$

G (Eq. (2)) is the third-order polynomial objective function, where $f_i^{(M)}$ is the ith muscle force; $n^{(M)}$ is the number of muscles, N_i is the muscle strength in the ith muscle. Eq. (3) defines the dynamic equilibrium equations for soft tissues, where C is a coefficient matrix, f is the soft tissues force, d is all external and internal force. Eq. (4) states that muscles can only pull, not push.

2.3. Data processing

Kinematic data obtained from the motion capture experiment were processed using Python (version 3.9.4) to detect the gait cycle and calculate joints ROM at frontal, transverse, and sagittal planes. Gait cycles were determined from the right hip motion curve: the start point of the gait cycle was the initial right heel strike with the ground (peak point of the curve), and the endpoint was the right heel again striking the ground (next peak point of the curve). The ROMs for the pelvis, hip, knee, and ankles joints were computed as the peak-to-peak change of the Euler angles of each gait cycle. Vertical excursion of the COM was also obtained based on the coordinate of COM in the sagittal plane. Step length and step width were obtained based on the coordinates of the left and right ankles joints in the sagittal and frontal planes at the support phase.

Kinetic data obtained from the musculoskeletal model were processed using Origin Pro (version 9.0, Microcal Software, Northampton, Massachusetts, USA) to extract the peak JRFs and muscle forces. JRFs included compressive force, anteroposterior (A-P) shear force, and mediolateral (M-L) shear force at the L4/L5, shoulder, hip, knee, and ankle joints. The resultant JRFs of compressive force, A-P shear force, and M-L shear force at each test joint were also calculated. Muscle force included trapezius, erector spinae, rectus abdominis, rectus femoris, biceps femoris, and tibialis anterior. The peak JRFs and muscle forces were both normalized to body weight (BW), and the results are shown as normalized dimensionless quantities.

The raw EMG data were processed using myoMUSCLE software (version 3.10, Noraxon, Scottsdale, Arizona, USA). They were full-wave filtered using an eighth-order Butterworth low pass filter (fc = 20-500 Hz) and then rectified and smoothed with the help of root mean square (RMS) calculation. Subsequently, the processed EMG signals were averaged to obtain the averaged EMG (AEMG) at the trapezius, erector spinae, rectus abdominis, rectus femoris, biceps femoris, and tibialis anterior.

Table 2
RMSE, SD and Pearson correlations between calculated and measured muscle forces. RMSE: root-mean-square deviation; r: Pearson's correlation coefficient; p: significant level

Index	Trapezius	Erector spine	Rectus abdominis	Rectus femoris	Biceps femoris	Tibialis anterior
RMSE	1.44	3.13	1.25	1.32	2.60	1.85
SD	2.88	3.22	2.37	2.31	2.72	1.88
r	0.682	0.564	0.705	0.787	0.526	0.580
p	0.000	0.020	0.000	0.000	0.000	0.001

2.4. Statistical analysis

In this study, the independent variables were the turnout ensemble (four levels), while the dependent variables included kinematic parameters (joint ROM, COM deviation, step length, and step width) and kinetic parameters (joint reaction force, muscle force, and EMG). Statistical tests were performed using the SPSS software (version 22, SPSS Inc., IBM, Armonk, NY, USA) with significance set at $p < 0.05$. All data were first tested for normality of distribution and homogeneity of variance using the Shapiro–Wilk test and the Levene test, respectively.

Quantitative kinematic and kinetic data were averaged, and standard deviations of the mean values were calculated for each test sample. A three-way repeated-measures analysis of variance (ANOVA) was performed on each measure to assess differences in the kinematics and kinetics between four test samples. Data were tested for sphericity, and if the assumption of sphericity was violated, Greenhouse–Geisser correction was used to adjust the degrees of freedom for the averaged tests of significance [19]. Bonferroni's post hoc analysis was performed to account for pairwise comparisons when the assumption of homogeneity of variance was accepted. If the equal variance assumption is violent during the ANOVA process, Dunnett's T3 test was performed for pairwise comparisons [20].

The developed models were validated by comparing calculated muscle forces and measured EMGs. The absolute agreement for all calculated muscle forces was performed using root-mean-square error (RMSE), and standard deviation (SD) for measured EMGs was also calculated. Pearson correlation coefficients (r) between the calculated muscle forces and measured EMGs were also calculated, categorized similarly to Taylor [21], as "weak" ($r \leq 0.35$) "moderate" ($0.35 < r \leq 0.67$), "strong" ($0.67 < r \leq 0.90$), and "excellent" ($r > 0.90$).

Grey relation analysis (GRA) was used to determine the kinematic index most strongly related to the kinetic index. GRA is a technique based on grey system theory to calculate the grey relational grade (r) of each comparison series to reference series according to the geometry similarity degree of the series curve. A comparison series with a higher r is more similar to the reference series and thus should be retained. Compared to the traditional mathematical analysis, GRA is more suitable for the nonlinear model and the small sample size. In this study, the reference series ($x_0(k)$) was the kinetic index that significantly differed among the four test samples. The comparison series ($x_i(k)$) was eighteen kinematic indexes obtained from the motion capture experiment

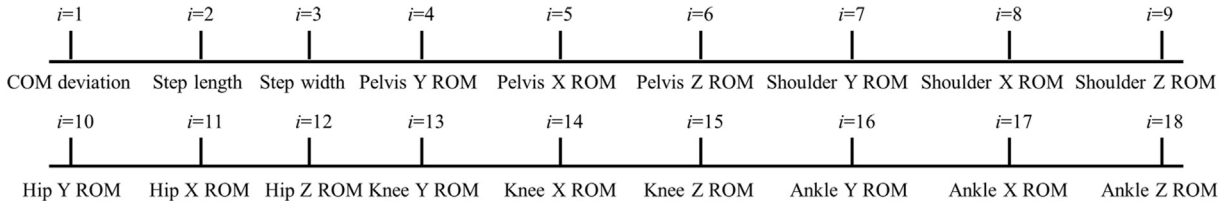

Fig. 4. The comparison series of eighteen kinematic index. X: frontal plane, Y: sagittal plane, Z: transverse plane.

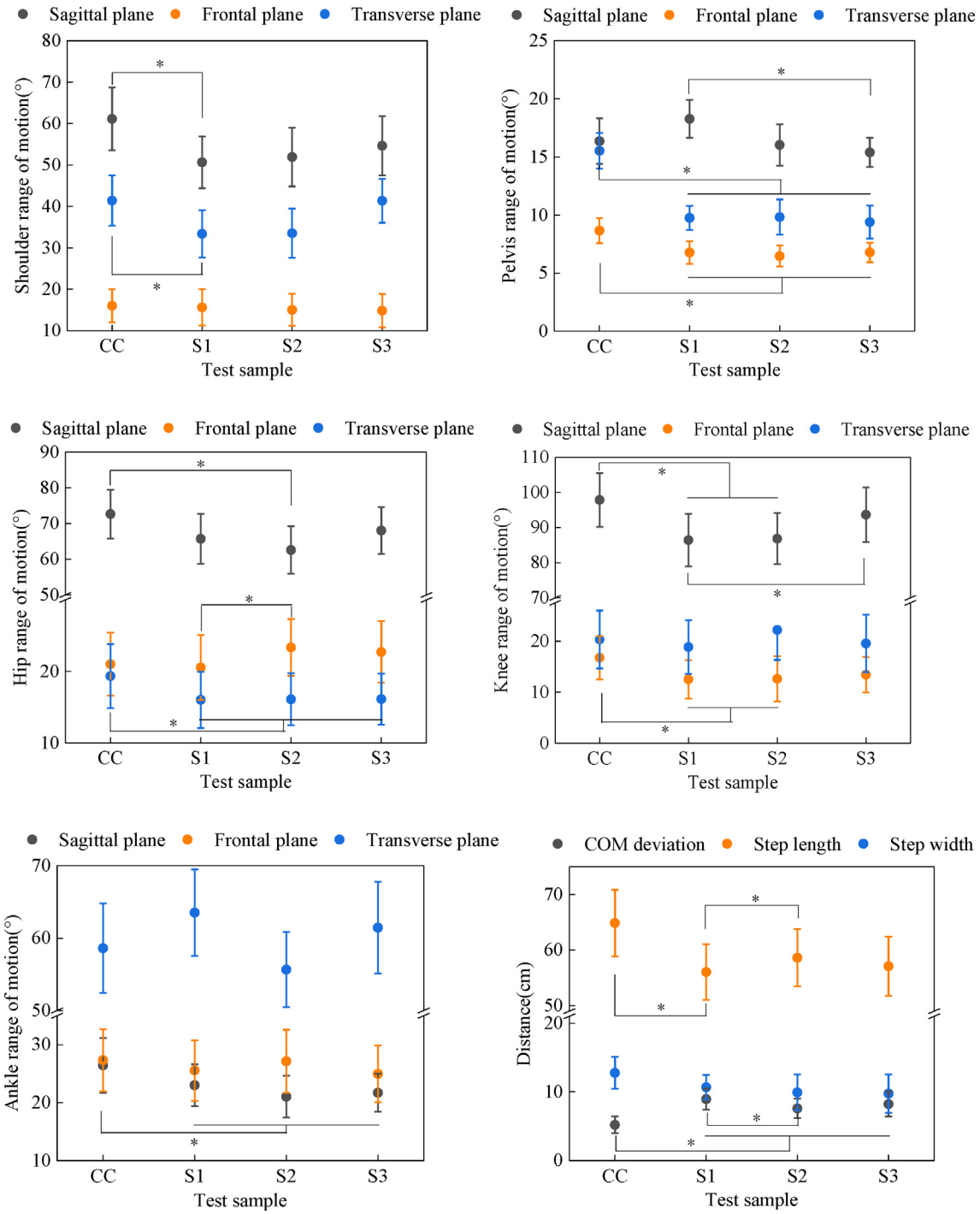

Fig. 5. Kinematic index in different test samples. *Indicates a significant difference.

(i = 1,2,3 …. .18, as shown in Fig. 4). k was the sample number (k = 1,2,3,4). The detailed steps were followed by Wu [22].

3. Results

3.1. Model validation

Table 2 presents the validation results for the calculated muscle forces using our musculoskeletal model versus the measured EMGs.

A significant correlation was found between calculated muscle forces and measured EMGs for all six test muscles. Strong correlation was found in the trapezius, rectus abdominis, and rectus femoris, with RMSE lower than the experimental SD. The erector spinae, biceps femoris, and tibialis anterior showed a moderate correlation with a lower RMSD than the experimental SD. In general, the calculated muscle forces using our musculoskeletal model quantitatively agreed with the measured EMGs.

3.2. Kinematics

Fig. 5 depicts the kinematic parameters during running with different test samples.

When running with the SCBA carriage, pelvis rotation and obliquity ROM were significantly reduced by 36.77–39.51% and

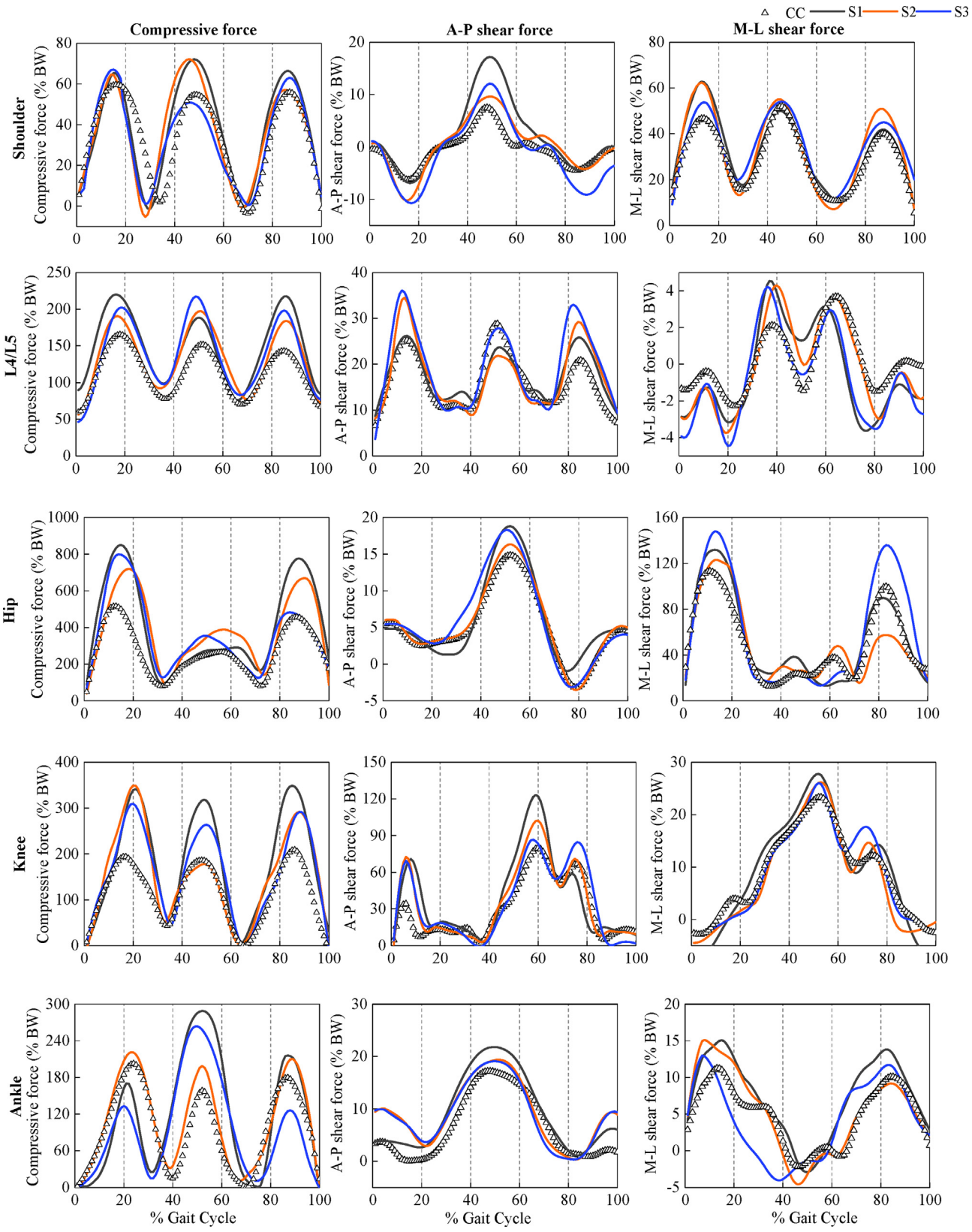

Fig. 6. The JRFs curve of shoulders, L4/L5, hip, knee, and ankle joints during one running gait. Results are shown as normalized dimensionless quantities. %BW: %body weight.

21.65–25.39%, respectively, (p = 0.00 and 0.01, respectively). A significant decrease of 7.34–9.87 cm in step length (p = 0.03) was also found with the increase in SCBA. COM was significantly shifted from 4.98 to 7.59–8.94 cm compared to the CC (p = 0.00).

A significant main effects due to the SCBA strap lengths were observed in pelvis tile ROM, hip adduction-abduction ROM, knee flexion-extension ROM, COM deviation, and step length ($p < 0.05$). COM deviation in S1 was 1.35 cm larger than in S2 (p = 0.04), and

hip adduction-abduction ROM and step length in S1 was 2.85° and 2.6 cm, respectively, lower than S2 ($p = 0.01$ and 0.03, respectively).

3.3. Kinetics

3.3.1. Joint reaction force (JRF)

Fig. 6 shows the JRF-time curve at the shoulder, L4/L5, hip, knee, and ankle joints during running with four test samples. Compressive force in all joints presented three peaks during a running gait. The maximum peak occurred at the toe-off phase, during which the body presented the maximum flexion or extensions.

Fig. 7 shows the mean of the peak JRFs and resultant JRFs predicted by the subject-specific musculoskeletal models. In all test joints, when compared to the CC, carrying SCBA significantly increased the peak compressive force, A-P shear force, and M-L shear force, respectively ($p < 0.05$). The resultant JRFs were used for detailed analysis, as shown in Fig. 7(D). The knee was exposed to the highest increase of resultant JRFs (an increase of 35.28–62.49%), followed by the hip (an increase of 33.31–52.5%), L4/L5 (an increase of 26.56–57.03%), and ankle (an increase of 10.46–39.96%), respectively, whereas the shoulder showed the lowest increase (an increase of 10.79–19.81%).

A significant main effect due to SCBA strap lengths was found for the resultant JRFs at the L4/L5, hip, and knee joints ($p < 0.05$). The maximum resultant JRFs were all reported for S1 among three SCBA strap lengths, which were 24.08% and 14.40% higher than S2 at the L4/L5 and hip joints, respectively ($p = 0.001$ and 0.007, respectively), and were 20.11% higher than S3 at the knee joint ($p = 0.002$).

3.3.2. Muscle forces

The force-time curve of six test muscles is shown in Fig. 8. Similar to the compressive force, the maximum peak occurred near the toe-off phase.

Fig. 9 shows the mean of the muscle force predicted by the musculoskeletal model. Compared to the CC, running with SCBA significantly increased the force for all six test muscles ($p < 0.05$). Rectus femoris increased most, from 81.84 %BW in the CC to 86.39–100.93 %BW ($p = 0.00$).

Significant main effects due to the SCBA strap lengths were observed for rectus abdominis, rectus femoris, and biceps femoris ($p < 0.05$). As expected, S1 had the maximum muscle force, 51.32% and 34.44% higher than S2 in rectus abdominis and rectus femoris, respectively ($p = 0.00$ and 0.00, respectively), while it was 26.68% higher than S3 in biceps femoris ($p = 0.01$).

3.4. Grey relational grade between kinematics and kinetics

Significant effects due to the SCBA carriage and strap lengths were observed on resultant JRFs at the L4/L5, hip, and knee ankle joint, as well as rectus abdominis, rectus femoris, and biceps femoris. These kinetic indexes were therefore selected as reference series in turn to determine their most related kinematic index.

As shown in Fig. 10, COM deviation was most likely correlated with the L4/L5 resultant JRF ($r_1 = 0.95$), while the pelvis tilt ROM ($r_4 = 0.93$) was highest correlated to rectus abdominis force. For the lower limb, step length was highest correlated to hip resultant JRF and rectus femoris ($r_2 = 0.94$ and 0.93, respectively). Knee flexion-extension ROM was highest correlated to knee resultant JRF and biceps femoris ($r_{13} = 0.96$ and 0.94, respectively).

4. Discussion

This study developed subject-specific musculoskeletal models for twelve subjects and analyzed the effects of SCBA carriage and strap lengths on their internal forces and the likelihood of potential MSDs. Referring to Fig. 5, the motion curve of the predicted JRFs showed reasonably good agreement with the previous studies [23]. The predicted muscle forces also showed good agreement with the measured EMG data. These results verified that our prediction on JRFs and muscle forces were reliable.

4.1. Effect of SCBA carrying on joint and muscle forces

Compared to the no-SCBA condition, carrying SCBA significantly increased internal forces in all test joints and muscles; however, the increased degree depended on the body segment. The most significant increase of JRFs occurred at the knee joint, followed by the hip joint. Similar to the results of JRFs, the rectus femoris and biceps femoris in the upper leg increased most with SCBA carriage. These results, which agreed with Unnikrishnan et al. [24] and Halder et al. [25], showed the contribution of lower limb forces while performing a load-carrying activity. It was also noted that the JRFs and muscle forces depended on the phase of the running cycle, and the highest forces generally occurred near the toe-off. This is because the unilateral leg was in maximum flexion or extension at this phase, resulting in the highest flexion or extension moment and muscle activations. The Finite-Element analysis demonstrated that greater JRFs in the lower limb might increase stress on the tibia's axial,

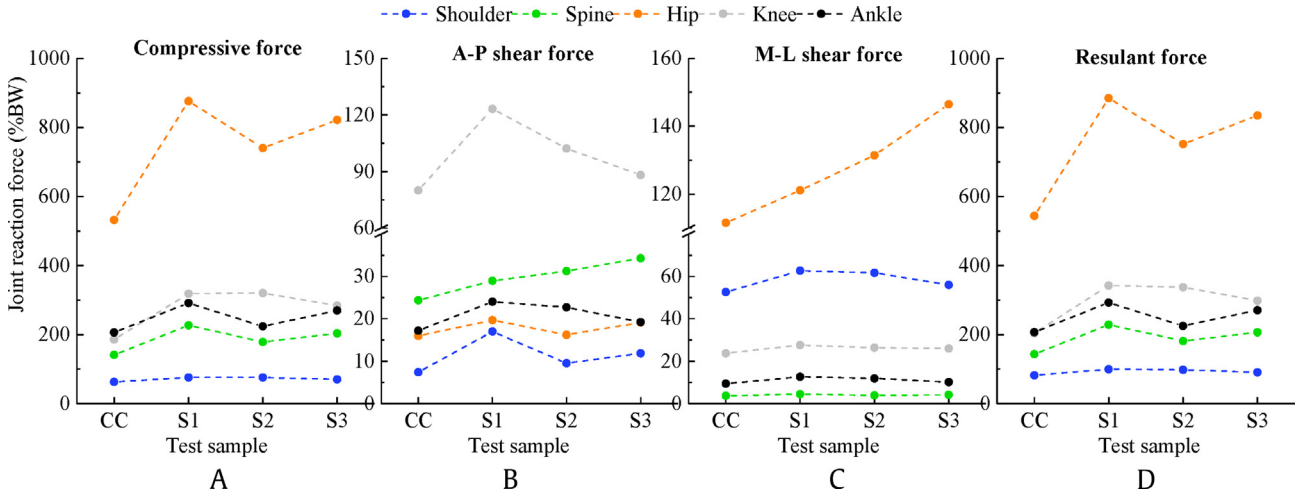

Fig. 7. The peak JRFs and resultant JRFs of shoulders, L4/L5 disc, hip, knee, and ankle joints during one running gait. (A) compressive force; (B) A-P shear force; (C) M-L shear force; (D) resultant JRFs. Results are shown as normalized dimensionless quantities. % BW: % body weight.

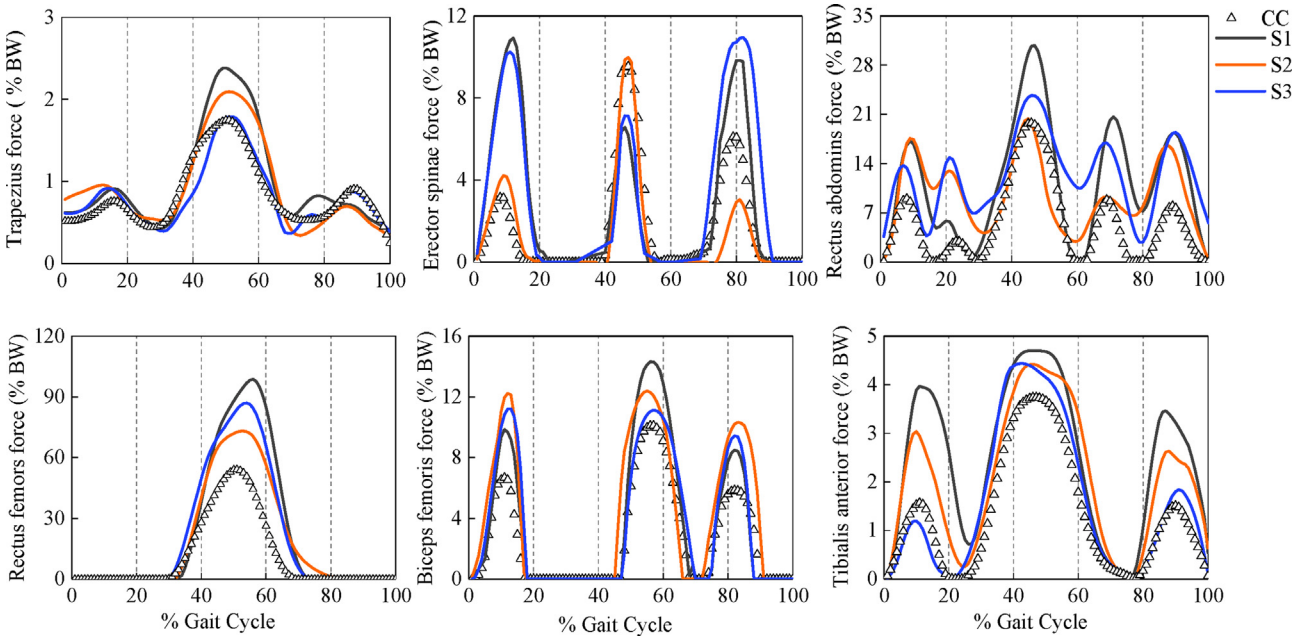

Fig. 8. The muscle force curves during one running gait. Results are shown as normalized dimensionless quantities. %BW: %body weight.

medial, or posterior aspects [26]. Higher contraction of the rectus femoris and the biceps femoris muscles could further increase high stress-time exposure in the anteroposterior region of the tibia [27].

Our musculoskeletal model also showed that carrying SCBA significantly increased the L4/L5 joint compressive force from 29.13% of the maximum admissible compressive lumbar force of 3400 N [27] to 37.6−48%, indicating the injury risk of low back pain increased by 8.48−18.89%. In addition, overstressed trunk muscle and imbalance exertion between the flexor and extensor muscles are prone to rapid muscle fatigue and then acute or overuse muscle strain [28]. By contrast, the shoulder JRF was least sensitive to SCBA carriage. This might be explained by the use of a hip belt that shifted the weight to the hip and lower back, therefore reducing the shoulder forces.

4.2. Effects of SCBA strap lengths on joint and muscle forces

Significant main effects due to strap lengths were observed for JRFs at L4/L5, hip and knee joints, as well as rectus abdominis, rectus femoris, and biceps femoris forces. From these results, variation of SCBA strap lengths was an efficient strategy to alter the newly recruited firefighters' loading in the lumbar spine and lower limb during load-carrying activities.

Interestingly, the changes in JRFs and muscle forces were not proportional to the increase or decrease in the SCBA strap lengths. The medium-fitting strap had minimum L4/L5 and hip JRFs and rectus femoris force, demonstrating a relative lower lumbar spine and hip loading. In contrast, loose-fitting straps caused the highest JRFs and muscle forces. For instance, the loose-fitting strap exerted more than 884 %BW of hip resultant JRF, far exceeding the 530 %BW of unloaded running [26]. Moreover, the peak L4/L5 compressive force was highest (1586N) in the loose-fitting strap, 46.64% of the threshold of 3400 N, indicating a moderate risk of low back pain. This might be explained by the pressure distribution at the shoulder and back under three strap lengths [29]. The loose-fitting strap meant that the SCBA bottle was farthermost away from the back, and there was less contact with the body. This would lead to uneven pressure distribution, increasing the exertion demand on the proximal torso. In the medium length, the straps were pulling more vertically, and the pressure may be well-distributed, therefore requiring less overall force. Currently, firefighters generally adjust strap lengths based on their convenience or habit. The above results indicated that a medium-fitting strap with 98−105 cm length was an appropriate solution.

4.3. Kinematic predictors of kinetic responses

The study also attempted to provide the predictors of kinetic response. GRA results demonstrated that COM deviation and pelvis tilt ROM were highly correlated to L4/L5 resultant JRF and rectus abdominis force, respectively. For every 1 cm increase in COM deviation, the L4/L5 resultant JRF increased about 20 %BW. For every 1 ° increase in pelvis forward, the rectus abdominis force increased about 13 %BW. COM deviation and pelvis forward lean are both related to postural balance. Therefore, it was concluded that the kinetic responses in the lumbar spine were mainly due to postural adjustment to maintain stability. Greater COM deviation and more pelvis forward lean may induce higher lumbar spine loading.

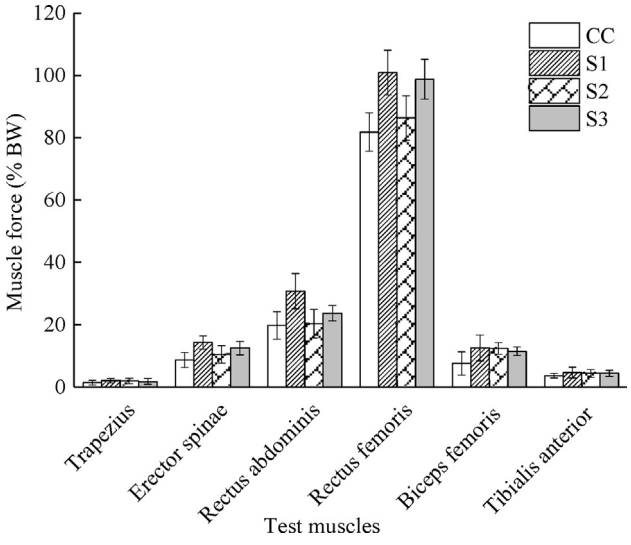

Fig. 9. The force of six test muscles during one running gait. Results are shown as normalized dimensionless quantities. %BW: %body weight.

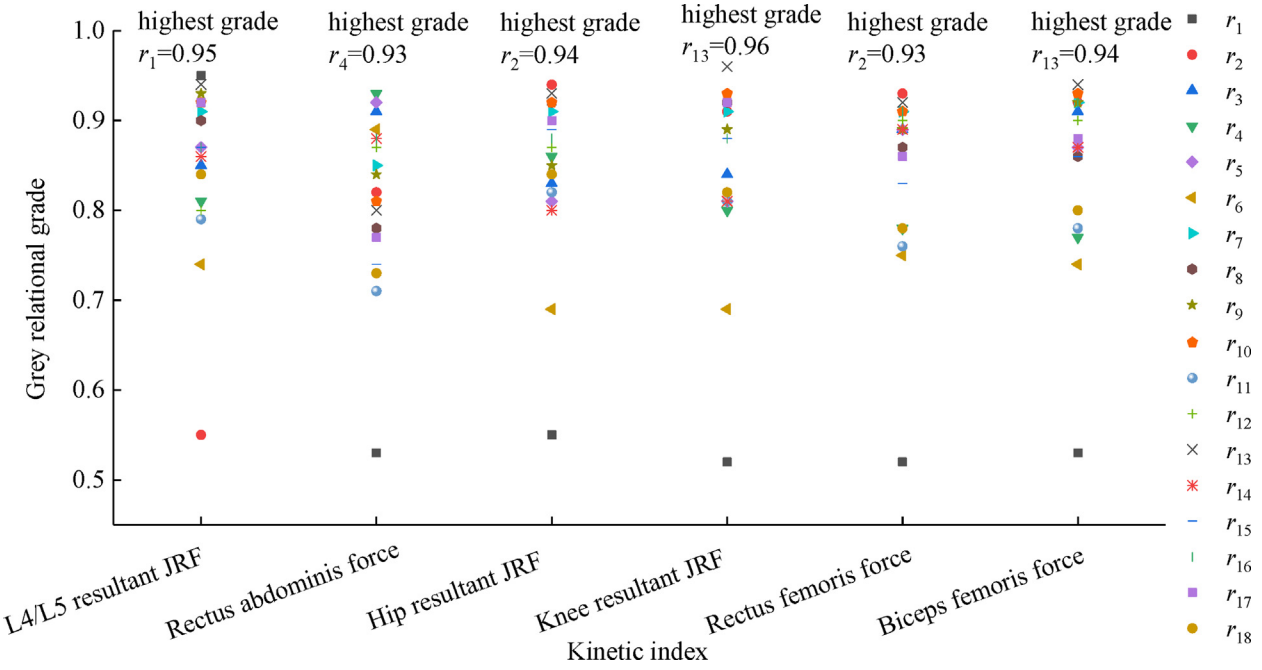

Fig. 10. Grey relational grade (r_i) between each kinetics with eighteen kinematic indexes.

The step length was highly correlated to the hip resultant JRF and rectus femoris force in the lower limb. For every 1 cm decrease in step length, the hip resultant JRF and rectus femoris force increased about 36.67 %BW and 1.77 %BW, respectively. By contrast, knee flexion-extension ROM showed the highest correlation to knee resultant JRF and biceps femoris. Every 1 ° decrease in knee flexion-extension would increase the knee resultant JRF and biceps femoris force by about 10.65 % BW and 2.5 % BW, respectively. These results indicated that shorter step length and less knee flexion-extension ROM might lead to a higher loading on the lower limb.

5. Limitation

The current study has some limitations that should be acknowledged. First, all risk factors of injury, such as running, load carriage, and abnormal kinematics, are mainly implicated with acute injuries; it was challenging to identify the varying relationship between MSDs and biomechanical factors with the increase of time. Second, the motion analysis data were collected in a laboratory environment; only a small sample of the newly recruited firefighters and a single type of test motion was discussed. Therefore, the results of this study may not represent all firefighters. Third, this is a biomechanical simulation, giving only kinematics and kinetics support as determinants of musculoskeletal symptoms. Future studies with a larger fire service population coupled with self-reported tests will likely provide more information.

6. Conclusion

Subject-specific musculoskeletal models were developed and validated to estimate full-body kinetic responses during SCBA carriage based on motion capture data. Model results revealed that the knee force was the most sensitive to SCBA carriage, followed by the rectus femoris and hip forces, indicating a potential risk of the tibia stress fracture. These results suggested that the training of the new recruits focuses on the coordinated movement of muscle and joints in the lower limb. The variation of SCBA straps length was verified as a feasible and convenient strategy to adjust loading at the lumbar spine and lower limb. A medium-fitting strap length of around 98–105 cm was recommended for the newly recruited firefighters with 172–178 cm height. Moreover, this study found that greater COM deviation and more pelvis forward lean may induce higher lumbar spine loading. In contrast, shorter step length and less knee flexion-extension may induce a higher loading on the lower limb.

Funding

Fundamental Research Funds for the Central Universities [Grant NO. 2232021G-08].

Conflicts of interest

The authors declare that they have no known competing financial interests or personal relationships that could have appeared to influence the work reported in this paper.

Acknowledgments

We express our gratitude to subjects for their kind support and experiment teachers for their technical support.

References

[1] Wang S, Park J, Wang Y. Cross-cultural comparison of firefighters' perception of mobility and occupational injury risks associated with personal protective equipment. Int J Occup Saf Ergon 2019;27(3):664–72.
[2] Shore E, Dally M, Brooks S, Ostendorf D, Newman M, Newman L. Functional movement screen as a predictor of occupational injury among denver firefighters. Saf Health Work 2020;11(3):301–6.
[3] Walton SM, Conrad KM, Furner SE, Samo DG. Cause, type, and workers' compensation costs of injury to fire fighters. Am J Ind Med 2003;43(4):454–8.
[4] Damrongsak M, Prapanjaroensin A, Brown KC. Predictors of back pain in firefighters. Workplace Health Saf 2018;66(2):61–9.
[5] Lee HJ, Oh JH, Yoo JR, Ko SY, Kang JH, Lee SK, Jeong W, Seong GM, Kang CH, Song SW. Prevalence of low back pain and associated risk factors among farmers in Jeju. Saf Health Work 2021;12(4):432–8.
[6] Punakallio A. Slip and fall risk among firefighters in relation to balance, muscular capacities and age. Saf Sci 2005;43:455–68.

[7] Martínez-fiestas M, Darmohraj A, Rodríguez-garz I, Delgado-padial A, Chumpitaz R. Voluntary and involuntary risk acceptance: a case study of firefighters. Saf Sci 2021;142:105394.
[8] Griefahn B, Künemund C, Bröde P. Evaluation of performance and load in simulated rescue tasks for a novel design SCBA: effect of weight, volume and weight distribution. Appl Ergon 2003;34(2):157–65.
[9] Hostler D, Pendergast DR. Respiratory responses during exercise in self-contained breathing apparatus among firefighters and nonfirefighters. Saf Health Work 2018;9(4):468–72.
[10] Pau M, Kim S, Nussbaumb MA. Fatigue-induced balance alterations in a group of Italian career and retained firefighters. Int J Ind Ergon 2014;44(5):615–20.
[11] Coca A, Kim JH, Duffy R, Williams WJ. Field evaluation of a new prototype self-contained breathing apparatus. Ergonomics 2011;54(12):1197–206.
[12] Kim MG, Seo J, Kim K, Ahn Y-S. Nationwide firefighter survey: the prevalence of lower back pain and its related psychological factors among Korean firefighters. Int J Occup Saf Ergon 2017;23(4):447–56.
[13] Katsavouni F, Bebetsos E, Antoniou P, Malliou P, Beneka A. Work-related risk factors for low back pain in firefighters. Is exercise helpful? Sport Sci Health 2014;10(1):17–22.
[14] Khurelbaatar T, Kim K, Lee SK, Kim YH. Consistent accuracy in whole-body joint kinetics during gait using wearable inertial motion sensors and in-shoe pressure sensors. Gait Posture 2015;42(1):65–9.
[15] Park H, Kakar RS, Pei J, Tome JM, Stull J. Impact of size of fire boot and SCBA cylinder on firefighters' mobility. Cloth Text Res J 2018;37(2):103–18.
[16] Skals S, Rasmussen KP, Bendtsen KM, Yang J, Andersen MS. A musculoskeletal model driven by dual Microsoft Kinect Sensor data. Multibody Syst Dyn 2017;41(4):1–20.
[17] Winter DA. Biomechanics and Motor Control of Human Movement. University of Waterloo Press; 1987.
[18] Karatsidis A, Jung M, Schepers HM, Bellusci G, Zee M De, Veltink PH, Andersen MS. Musculoskeletal model-based inverse dynamic analysis under ambulatory conditions using inertial motion capture. Med Eng Phys 2019;65:68–77.
[19] Zhang Z, Tang X. Effect of fiber type, water content, and velocity on wetness perception by the volar forearm test: stimulus intensity test. Perception 2019;49(2):139–54.
[20] Lee S, Lee DK. What is the proper way to apply the multiple comparison test? Korean J Anesthesiol 2018;(5):353–60.
[21] Taylor R. Interpretation of the correlation coefficient: a basic review. J Diagnostic Med Sonogr 1990;1:35–9.
[22] Wu H. A comparative study of using grey relational analysis in multiple attribute decision making problems. Qual Eng 2002;15(2):209–17.
[23] Kathawala KJ. Effects of Slips and Trips on Resultant Lumbar Kinematics, Lumbar Muscle Activity and Low-Back Loads. Rochester Institute of Technology; 2018.
[24] Unnikrishnan G, Xu C, Baggaley M, Tong J, Kulkarni S, Edwards WB. Effects of body size and load carriage on lower-extremity biomechanical responses in healthy women. BMC Musculoskelet Disord 2021;22(219):1–11.
[25] Halder A, Nordin A, Miller M, Kuklane K, Nirme J. Effects of leg fatigue due to exhaustive stair climbing on gait biomechanics while walking up a 10° incline – implications for evacuation and work safety. Fire Saf J 2021;123:103342.
[26] Xu C, Silder A, Zhang J, Reifman J, Unnikrishnan G. A cross-sectional study of the effects of load carriage on running characteristics and tibial mechanical stress: implications for stress-fracture injuries in women. BMC Musculoskelet Disord 2017;18(125):1–12.
[27] Neesham-smith D, Aisbett B, Netto K. Trunk postures and upper-body muscle activations during physically demanding wildfire suppression tasks. Ergonomics 2013;57(1):86–92.
[28] Gómez L, Díaz CA, Orozco GA, García JJ. Dynamic analysis of forces in the lumbar spine during bag carrying. Int J Occup Saf Ergon 2017;(8):1–34.
[29] Knapik J, Harman E, Reynolds K. Load carriage using packs: a review of physiological, biomechanical and medical aspects. Appl Ergon 1996;27(3):207–16.